Journal of Computational and Applied Mathematics 234 (2010) 1161–1171

Contents lists available at ScienceDirect

Journal of Computational and Applied Mathematics

journal homepage: www.elsevier.com/locate/cam

A reliable algorithm to solve 3D frictional multi-contact problems: Application to granular media

Issa Sanni [1], Emmanuel Bellenger *, Jérôme Fortin, Patrice Coorevits

Laboratoire de Technologies Innovantes (EA - 3899), Université de Picardie, IUT de l'Aisne, 48 rue d'Ostende, 02100 Saint-Quentin, France

ARTICLE INFO

Article history:
Received 25 September 2008
Received in revised form 26 June 2009

Keywords:
Non-smooth frictional contact
Granular media
Multi-contact problems
Discrete element method

ABSTRACT

We present in this paper an improved non-smooth Discrete Element Method (DEM) in 3D based on the Non-Smooth Contact Dynamics (NSCD) method. We consider a three-dimensional collection of rigid particles (spheres) during the motion of which contacts can occur or break. The dry friction is modeled by Coulomb's law which is typically non-associated. The non-associativity of the constitutive law poses numerical challenges. By adopting the use of the bi-potential concept in the framework of the NSCD DEM, a faster and more robust time stepping algorithm with only one predictor-corrector step where the contact and the friction are coupled can be devised. This contrasts with the classical method where contact and friction are treated separately leading to a time stepping algorithm that involves two predictor-corrector steps. The algorithm has been introduced in a 3D version of the NSCD DEM software MULTICOR. Numerical applications will show the robustness of the algorithm and the possibilities of the MULTICOR software for solving three-dimensional problems.

1. Introduction

The behavior of granular assemblies is of central importance for a large number of engineering disciplines, finding applications in soil mechanics, material handling and powder technology, to name a few. It is the complex range of behavior that makes granular material difficult to understand and explain why modeling such material is still a challenge. In the numerical area, the Discrete Element Method (DEM) which takes into account the discrete character of granular materials has been pioneered in [1,2]. The name DEM refers to the fact that the method considers the granular material as a system of individual particles and not as a continuum. When contact occurs between particles, a local constitutive law determines the inter-particle contact forces and consequently the resulting motions of the particles involved in the contact. Among the DEM, one can distinguish the smooth DEM from the non-smooth DEM.

In the smooth DEM, a smooth interaction law between particles is used. The pioneers of this method are Cundall and Strack [1,2]. Interaction laws allow particles to interpenetrate each other. The most popular is the spring-dashpot model, which consists of a spring to provide the repulsive force and a dashpot to dissipate a portion of energy. The results obtained are less accurate but approximating equations are smoother resulting in a better convergence.

In the non-smooth DEM, granular materials are more realistically modeled by a system of particles that do not interpenetrate and are subjected to friction and shocks with restitution coefficients. Thus, this approach is described as non-smooth. The interaction laws between grains are no longer smooth (non-differentiable) and the velocity is not continuous with respect to the time (some jumps occur during the shocks). The Non-Smooth Contact Dynamics (NSCD) method, initiated

* Corresponding author.
E-mail address: emmanuel.bellenger@u-picardie.fr (E. Bellenger).

[1] In memory of our friend and colleague Issa Sanni, 1975-2007.

0377-0427/$ – see front matter © 2009 Elsevier B.V. All rights reserved.
doi:10.1016/j.cam.2009.07.015

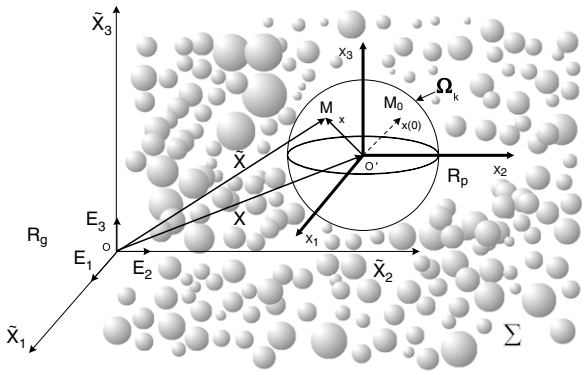

Fig. 1. Configuration of the system.

in [3,4] is more general. The contact between particles is modeled by Coulomb's unilateral contact law with dry friction. With this method, multiple contacts and shocks between particles or multibody systems can be taken into account [5,6]. The non-smoothness of the equations is the source of numerical difficulties. Computing time increases rapidly in accordance with the number of contacts. These technical difficulties make the simulation of system with a large number of particles hard.

We present in this paper an improved non-smooth DEM based on the NSCD method. We consider a three-dimensional collection of rigid particles (spheres) during the motion of which contacts can occur or break. The dry friction is modeled by Coulomb's law which is typically non-associated: during the contact, the sliding vector is not normal to the friction cone. The non-associativity of the constitutive law poses numerical challenges. The main feature of our algorithm is to overcome this kind of difficulty by means of the bi-potential theory [7]. More precisely, by adopting a variational inequality-based formulation of the frictional contact law, its time-integration is reduced to a single predictor corrector step. This contrasts with the classical method where contact and friction are treated separately leading to a time stepping algorithm that involves two predictor-corrector steps: one for the contact problem and another for the friction problem [8]. The MULTICOR software so developed [9] is based on a NSCD model. At each time step, an iterative algorithm is used to compute the values of the variables at the end of the step. In the local stage, for each particle, the forces are computed from the relative displacements using an interaction law with the bi-potential concept, which models the frictional contact and shocks. In the global stage, Newton's second law is used to determine, for each particle, the resulting acceleration, which is then time-integrated to find the new particle positions. This process is repeated until the simulation is achieved.

Numerical applications will show the robustness of the algorithm and the possibilities of the MULTICOR software for solving three-dimensional problems.

2. Configuration of the system and equations of motion

The DEM consists in modeling the granular media as a system of discrete particles (the grains) where the forces governing particle motion reduce to gravity and inter-grain contact forces. In three dimensions, the grains are considered as rigid spherical particles.

We consider a dry granular material modeled by a system $\Sigma = \bigcup_{k=1}^{p} \Omega_k$ of p rigid spheres Ω_k. The system Σ can be classically parameterized by the generalized coordinates (degrees of freedom) $\mathbf{q} = (q_1, q_2, \ldots, q_n)$, with $n = 6p$.

The bodies interact between themselves and with the boundaries according to unilateral constraints specified by Signorini conditions and Coulomb's frictional law. In the following, we present a description of the state of the mechanical system using generalized coordinates and recall the equations of motion using Lagrangian formulation.

Let $\langle \tilde{X_1}, \tilde{X_2}, \tilde{X_3} \rangle$ and $\langle x_1, x_2, x_3 \rangle$ be a system of coordinates relative to a global orthonormal frame $R_g = (O; E_1, E_2, E_3)$ and to the local frame $R_b = (O'; t_1, t_2, t_3)$ respectively, where O' denotes the center of gravity of Ω_k (Fig. 1).

Thus, a current point M of the rigid body Ω_k depends on the time t through $\overrightarrow{O'M} = \mathbf{R}(t)\overrightarrow{O'M_0}$, where M_0 denotes the position of M at time $t = 0$, and $\mathbf{R}(t)$ the rotation matrix defined by Euler's angles $(\psi(t), \theta(t), \varphi(t))$.

For a rigid body, the matrix of the generalized coordinates is then:

$$\mathbf{q} = (x_1(t), x_2(t), x_3(t), \psi(t), \theta(t), \varphi(t)). \tag{1}$$

The position and velocity of any point M of a body Ω_k can be respectively written;

$$\tilde{\mathbf{X}}(t) = \mathbf{X}(t) + \mathbf{R}(t)(\tilde{\mathbf{X}}(0) - \mathbf{X}(0)), \qquad \dot{\tilde{\mathbf{X}}}(t) = \dot{\mathbf{X}}(t) + j(\mathbf{w})(\tilde{\mathbf{X}}(t) - \mathbf{X}(t)) \tag{2}$$

where $\mathbf{X}(t)$ and $\tilde{\mathbf{X}}(t)$ denote at time t the position in R_g of the center of gravity of Ω_k, and the position of M respectively. With $j(\mathbf{w}) = \dot{\mathbf{R}}(t)^{\mathbf{t}}\mathbf{R}(t)$, where $j(\mathbf{x})$ denotes the "operator of cross-product operator by $\mathbf{x}$" defined by $j(\mathbf{x})(\mathbf{y}) \equiv \mathbf{x} \wedge \mathbf{y}$.

To study a mechanical system composed of rigid bodies with a finite number of degrees of freedom, it is necessary to be able to characterize their positions in a reference coordinate system. Moreover, bodies cannot move freely since they cannot

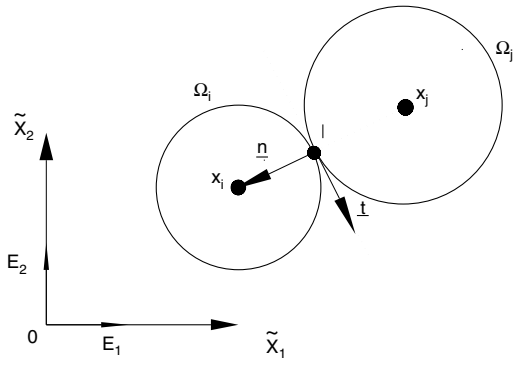

Fig. 2. Local coordinate system.

penetrate each other (contact law). Classically, the generalized coordinates vector $\mathbf{q}$, collecting the independent position of mass center and angular rotation of all rigid bodies, is associated to any position of the system Σ. Then, at each time, the position of a point M of Σ defined in (2) is determined by the n variables $(q_1, q_2, \ldots, q_n)$.

If we denote by k the number of contacts between rigid bodies and boundaries, the total number of unknowns is $6p + 2k$ with $2k$ corresponding to normal and tangential forces. The two components of the tangential force will be deduced from knowing the global tangential force determined from the tangential velocity and the normal force. Therefore, while the total number of unknowns is $6p + 2k$, the number of equations of the dynamics is $6p$. In this configuration, the dynamics system governed by Newton's second law is written here as:

$$\mathbf{M}\ddot{\mathbf{q}} = \mathbf{F} + \sum_{c=1}^{k} \mathbf{Q}^c, \tag{3}$$

where F denotes the generalized forces associated to the external forces applied to Σ, and $\mathbf{Q}^c$ the generalized forces associated to the contact forces summed on all the contacts k. $\mathbf{M}$ is a symmetric positive definite $n \times n$ matrix.

Thus, $2k$ additional equations are needed in order to solve the problem. These equations are given by relations that describe interaction between bodies.

2.1. The complementary relations (contact law) and local variables

Eq. (3) is general and we must now specify the number of contacts and the modeling of the contact between the solids Ω_k. So let us assume that Σ which has a priori n degrees of freedom is subjected to k supplementary relations between the bodies. When the interactions are modeled by unilateral contact between bodies, where contacts can occur or break, we can write the interaction law as follows:

$$\text{law}(\dot{\mathbf{u}}, \mathbf{r}) = .\text{TRUE.} \quad (c = 1, 2, \ldots, k) \tag{4}$$

where the local relative velocity $\dot{\mathbf{u}}$ and the contact reaction $\mathbf{r}$ are the chosen variables to describe the contact. The system to solve then becomes:

$$\mathbf{M}\ddot{\mathbf{q}} = \mathbf{F} + \sum_{c=1}^{k} \mathbf{Q}^c, \tag{5}$$

$$\text{law}(\dot{\mathbf{u}}, \mathbf{r}) = .\text{TRUE.} \quad (c = 1, 2, \ldots, k). \tag{6}$$

This system must be completed with the kinematic relations $\dot{\mathbf{u}} = {}^t\mathbf{P}\dot{\mathbf{q}}$ and $\mathbf{r} = {}^t\mathbf{P}\mathbf{Q}^c$ (see Section 2.2) which link the dual variables of (6) to the generalized coordinates and forces involved in (5). The matrix $\mathbf{P}$ depends on the geometry of the grains and the orientation of the contacts.

2.2. Expression of the $\mathbf{P}$ matrix

Let Ω_i and Ω_j be two bodies in contact at a point I for some value of the time (see Fig. 2 given in two dimensions). The instantaneous velocity of the particles Ω_i and Ω_j passing at point I are respectively $\dot{\mathbf{u}}_i$ and $\dot{\mathbf{u}}_j$. The relative velocity is then $\dot{\mathbf{u}} = \dot{\mathbf{u}}_i - \dot{\mathbf{u}}_j$. Let $\mathbf{r}$ be the contact reaction acting at I from Ω_j onto Ω_i. To each couple Ω_i and Ω_j, candidate to contact, is associated a local basis $(\mathbf{n}, \mathbf{s}, \mathbf{t})$. $\mathbf{n}$ denotes the normal unit vector orthogonal at point I directed towards Ω_i. $\mathbf{s}$ and $\mathbf{t}$ are the unit tangent vectors at point I (Fig. 2). $\mathbf{T}$ is the matrix of basis change between R_g and the local basis $(\mathbf{n}, \mathbf{s}, \mathbf{t})$.

Thus any element $\dot{\mathbf{u}}$ and $\mathbf{r}$ may be decomposed into the form

$$\dot{\mathbf{u}} = \dot{\mathbf{u}}_t + \dot{\mathbf{u}}_s + \dot{u}_n\mathbf{n}, \qquad \mathbf{r} = \mathbf{r}_t + \mathbf{r}_s + r_n\mathbf{n} \tag{7}$$

where $\dot{u}_n$ is the normal velocity, $\dot{\mathbf{u}}_t$ the sliding velocity according to $\mathbf{t}$ axis, $\dot{\mathbf{u}}_s$ the sliding velocity according to $\mathbf{s}$ axis, r_n the normal contact reaction or contact pressure, $\mathbf{r}_t$ and $\mathbf{r}_s$ the friction forces or resistance forces to sliding.

According to (2), the relative velocity of body Ω_i compared to body Ω_j is given by:

$$\dot{\tilde{\mathbf{X}}}_{ij} = \dot{\mathbf{X}}_i + j(\mathbf{w}_i)(\tilde{\mathbf{X}}_i - \mathbf{X}_i) - \dot{\mathbf{X}}_j - j(\mathbf{w}_j)(\tilde{\mathbf{X}}_j - \mathbf{X}_j). \tag{8}$$

For the spherical particles in contact at a point on the surface, we can write:

$$\dot{\tilde{\mathbf{X}}}_{ij} = \left(\mathbf{I}\ a_i j(\mathbf{n})\ \ - \mathbf{I}\ a_j j(\mathbf{n})\right)(\dot{\mathbf{q}}), \tag{9}$$

where a_i and a_j denote the radii of the bodies Ω_i and Ω_j respectively and $j(\mathbf{n})$ has been defined in (2).

By projecting (9) on the local basis $(\mathbf{n}, \mathbf{s}, \mathbf{t})$, we obtain a relation between the local relative velocity $\dot{\mathbf{u}} = {}^{\mathbf{t}}\mathbf{T}\dot{\tilde{\mathbf{X}}}_{ij}$ and the generalized velocities of the two bodies candidates to the contact $\dot{\mathbf{q}}$, given by the matrix ${}^{\mathbf{t}}\mathbf{P}$ [9].

$$\dot{\mathbf{u}} = {}^{\mathbf{t}}\mathbf{P}\dot{\mathbf{q}} \quad \text{with } {}^{\mathbf{t}}\mathbf{P} = {}^{\mathbf{t}}\mathbf{T}\left(\mathbf{I}\ a_i j(\mathbf{n})\ \ - \mathbf{I}\ a_j j(\mathbf{n})\right). \tag{10}$$

Then the interaction law (4) is now written between the local relative velocity $\dot{\mathbf{u}}$ and the local contact reaction $\mathbf{r}$. By projecting $\mathbf{r}$ on to the global frame by using the relation $\mathbf{r} = {}^{\mathbf{t}}\mathbf{P}\mathbf{Q}^c$, we obtain $\mathbf{Q}^{\mathbf{c}}$ the generalized force associated to the contact reaction $\mathbf{r}$.

3. Coulomb's contact law with dry friction based on a bi-potential

As mentioned before, the spherical bodies are assumed to be rigid and cannot overlap. We assume that contacting bodies Ω_k interact according to Coulomb's unilateral contact law with dry friction. This dissipative non-linear law can be written:

$$\begin{array}{ll} \text{if } r_n = 0 \text{ then } \dot{u}_n \geq 0 & \text{no contact,} \\ \text{if } r_n > 0 \text{ and } \|\mathbf{r}_T\| < \mu r_n \text{ then } \dot{\mathbf{u}} = \mathbf{0} & \text{contact with sticking,} \\ \text{if } r_n > 0 \text{ and } \|\mathbf{r}_T\| = \mu r_n & \text{contact with sliding.} \\ \text{then } \dot{u}_n = 0,\ \exists \dot{\lambda} \geq 0 \text{ such as } \dot{\mathbf{u}}_T = -\dot{\lambda}\dfrac{\mathbf{r}_T}{\|\mathbf{r}_T\|} & \end{array} \tag{11}$$

where $\mathbf{r}_T = \mathbf{r}_t + \mathbf{r}_s$ and $\dot{\mathbf{u}}_T = \dot{\mathbf{u}}_t + \dot{\mathbf{u}}_s$ denote the tangential components of the contact reaction and the relative velocity respectively. Let K_μ be the Coulomb's friction cone which defines the set of admissible forces:

$$K_\mu = \{(r_n, \mathbf{r}_T) \text{ such as } \|\mathbf{r}_T\| - \mu r_n \leq 0\} \tag{12}$$

where $\|\|$ and μ denote the euclidian norm of $\mathbb{R}^3$ and the friction coefficient respectively. Then the inverse contact law can be written:

$$\begin{array}{ll} \text{if } \dot{u}_n > 0 \text{ then } \mathbf{r} = \mathbf{0} & \text{no contact,} \\ \text{if } \dot{\mathbf{u}} = \mathbf{0} \text{ then } \mathbf{r} \in K_\mu & \text{contact with sticking,} \\ \text{if } -\dot{\mathbf{u}}_T < 0 \text{ then } r_n > 0 \text{ and } \mathbf{r}_T = -\mu r_n \dfrac{\dot{\mathbf{u}}_T}{\|\dot{\mathbf{u}}_T\|} & \text{contact with sliding.} \end{array} \tag{13}$$

It is clear from geometrical considerations that the relative velocity $\dot{\mathbf{u}}$ is not normal to Coulomb's cone, because the normal relative $\dot{u}_n$ is equal to zero. This observation indicates that normality does not apply. Therefore, for the frictional contact law, an associated formulation does not exist in terms of a sub-differential using a pseudo-potential of the type $-\dot{\mathbf{u}} \in \partial\Psi_{K_\mu}(\mathbf{r})$. De Saxcé and Feng [10] have shown that this complete contact law can be written in the form of the following differential equation:

$$-(\dot{\mathbf{u}}_T + (\dot{u}_n + \mu\|\dot{\mathbf{u}}_T\|)\mathbf{n}) \in \partial\Psi_{K_\mu}(\mathbf{r}). \tag{14}$$

The behavior of materials admitting this kind of constitutive law is qualified as non-standard or non-associated. By developing the previous relation, de Saxcé has shown that the contact law along with its inverse, can be obtained by applying the normality rule to a function, called bi-potential, which depends on both dual variables. For the complete contact law with dry friction, de Saxcé et al. proposed to introduce a bi-potential as follows:

$$\begin{array}{l} b_c : V \times F \to \mathbb{R} \\ (-\dot{\mathbf{u}}, \mathbf{r}) \mapsto b_c(-\dot{\mathbf{u}}, \mathbf{r}) = \Psi_{\mathbb{R}^-}(-\dot{u}_n) + \Psi_{K_\mu}(\mathbf{r}) + \mu r_n\| - \dot{\mathbf{u}}_T\| \end{array} \tag{15}$$

where V and F denote respectively the spaces of generalized velocities and forces, put in duality through the scalar product of $\mathbb{R}^3$. The condition of non inter-penetrability $\dot{u}_n \geq 0$ (see Fig. 3) is represented by the indicatory function of $\mathbb{R}^-$, noted $\Psi_{\mathbb{R}^-}(-\dot{u}_n)$, which is equal to zero when $-\dot{u}_n \leq 0$ and to $+\infty$ otherwise. The contact bi-potential also takes infinite values if the condition $\mathbf{r} \in K_\mu$ is not satisfied.

This bi-potential of the contact is bi-convex (convex with respect to each of the variables) and satisfies [7,10]:

$$\forall -\dot{\mathbf{u}}, \mathbf{r} \in \mathbb{R}^3, \quad b_c(-\dot{\mathbf{u}}, \mathbf{r}) \geq -\dot{\mathbf{u}}.\mathbf{r}. \tag{16}$$

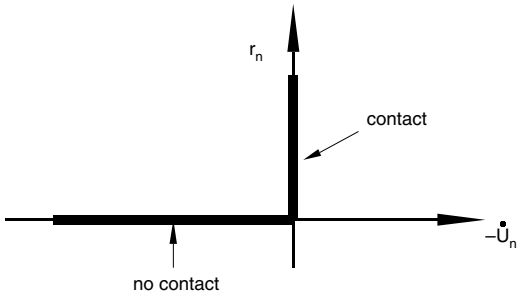

Fig. 3. The unilateral contact law.

Moreover, the couples for which the equality is reached in the previous relation, are called extremal couples:

$$b_c(-\dot{\mathbf{u}}, \mathbf{r}) = -\dot{\mathbf{u}}.\mathbf{r} \Leftrightarrow \mu r_n \|-\dot{\mathbf{u}}_T\| = -(\dot{\mathbf{u}}_T.\mathbf{r}_t + \dot{u}_n r_n). \tag{17}$$

These couples verify Coulomb's unilateral contact law with dry friction (11) and the inverse law (13), which can be written implicitly:

$$-\dot{\mathbf{u}} \in \partial_r b_c(-\dot{\mathbf{u}}, \mathbf{r}), \qquad \mathbf{r} \in \partial_{-\dot{\mathbf{u}}} b_c(-\dot{\mathbf{u}}, \mathbf{r}) \tag{18}$$

where $\partial_x b_c$ denotes the sub-differential of b_c with respect to the variable x.

4. Local resolution of the contact law

The classical formulation of the unilateral contact problem with dry friction needs two variational inequalities. The first inequality expresses the unilateral contact condition and the second the friction one. Based on this formulation, efficient predictor-corrector algorithms have been proposed in the literature [8]. Basically such algorithms solve alternatively the contact and the friction problems until convergence. As a consequence, two predictor-corrector steps are required. By adopting the use of the bi-potential, a faster and more robust time stepping algorithm with only one predictor-corrector step where the contact and the friction are coupled can be devised. This formulation is quite general and well suited for non-standard behaviors admitting a bi-potential. For the resolution of the unilateral contact law with the bi-potential formalism, we use the augmented Lagrangian method [11]. First, let us write relation (18) as follows:

$$\forall \mathbf{r}' \in K_\mu, \quad b_c(-\dot{\mathbf{u}}, \mathbf{r}') - b_c(-\dot{\mathbf{u}}, \mathbf{r}) \geq -\dot{\mathbf{u}}(\mathbf{r}' - \mathbf{r}). \tag{19}$$

During the local stage, the relative velocity $\dot{\mathbf{u}}$ is given for each contact. The aim is now to find the corresponding contact reaction $\mathbf{r}$, solution of (19). Let us choose a positive arbitrary coefficient ρ, whose value will be fixed later to ensure the numerical convergence of the algorithm [9]. Then inequality (19) can be written:

$$\forall \mathbf{r}' \in K_\mu, \quad \rho b_c(-\dot{\mathbf{u}}, \mathbf{r}') - \rho b_c(-\dot{\mathbf{u}}, \mathbf{r}) + [\mathbf{r} - (\mathbf{r} + \rho(-\dot{\mathbf{u}}))].(\mathbf{r}' - \mathbf{r}) \geq 0. \tag{20}$$

Using now the definition (15) of the contact bi-potential, relation (20) becomes with $\dot{u}_n \geq 0$ and $\mathbf{r} \in K_\mu$:

$$\forall \mathbf{r}' \in K_\mu, \quad (\mathbf{r} - \boldsymbol{\tau}).(\mathbf{r}' - \mathbf{r}) \geq 0 \tag{21}$$

where $\boldsymbol{\tau} = \mathbf{r} - \rho[\dot{\mathbf{u}}_T + (\dot{u}_n + \mu\|-\dot{\mathbf{u}}_T\|).\mathbf{n}]$ denotes the augmented reaction. Relation (21) implies that $\mathbf{r}$ is the projection of $\boldsymbol{\tau}$ onto the Coulomb's cone ($\mathbf{r} = \text{proj}(\boldsymbol{\tau}, K_\mu)$).

It can be solved with a Usawa-like algorithm. Indeed, let $(-\dot{\mathbf{u}}^i, \mathbf{r}^i)$ be an approximation of $(-\dot{\mathbf{u}}, \mathbf{r})$ at the iteration i. Then the calculus of $\mathbf{r}^{i+1}$ is decomposed into one predictor-corrector step:

$$\begin{aligned} &\text{Predictor}: \quad \boldsymbol{\tau}^{i+1} = \mathbf{r}^i - \rho[\dot{\mathbf{u}}_T^i + (\dot{\mathbf{u}}_n^i + \mu\|-\dot{\mathbf{u}}_T^i\|).\mathbf{n}], \\ &\text{Corrector}: \quad \mathbf{r}^{i+1} = \text{proj}(\boldsymbol{\tau}^{i+1}, K_\mu). \end{aligned} \tag{22}$$

The projection onto the Coulomb's cone, which corresponds to the correction step of the scheme (22), leads to the three following events:

$$\begin{aligned} &\text{if } \boldsymbol{\tau}^{i+1} \in K_\mu^*, && \text{no contact,} \\ &\text{if } \boldsymbol{\tau}^{i+1} \in K_\mu, && \text{contact with sticking,} \\ &\text{if } \boldsymbol{\tau}^{i+1} \in \mathbb{R}^3 - (K_\mu \cup K_\mu^*) && \text{contact with sliding,} \end{aligned} \tag{23}$$

where K_μ^*, the dual of the Coulomb's cone, is defined by:

$$K_\mu^* = \{(\dot{u}_n, \dot{\mathbf{u}}_T) \text{ such as } \mu\|\dot{\mathbf{u}}_T\| + \dot{u}_n \leq 0\}. \tag{24}$$

The corrector step requires computing the project of the prediction and can be reformulated as solution of the convex non-linear programming problem with constraints (25) which is transformed into an unconstrained minimization problem by means of the Lagrange multipliers technique ([11]).

$$\mathbf{r}^{i+1} = \inf_{\mathbf{r}^{i+1}\in K_\mu} \frac{1}{2}\|\mathbf{r}^{i+1} - \boldsymbol{\tau}^{i+1}\|^2. \tag{25}$$

Moreover, one of the great interests of this formulation, is that the projection onto the Coulomb's cone can be calculated analytically as follows:

$$\begin{aligned}
&\text{if } \mu\|\boldsymbol{\tau}_T^{i+1}\| \le -\tau_n^{i+1} \text{ then } \mathbf{r}^{i+1} = 0 && \text{separating out,}\\
&\text{if } \|\boldsymbol{\tau}_T^{i+1}\| < \mu\tau_n^{i+1} \text{ then } \mathbf{r}^{i+1} = \boldsymbol{\tau}^{i+1} && \text{contact with sticking,}\\
&\text{else } \mathbf{r}^{i+1} = \boldsymbol{\tau}^{i+1} - \left(\frac{\|\boldsymbol{\tau}_T^{i+1}\| - \mu\tau_n^{i+1}}{(1+\mu^2)}\right)\left(\frac{\boldsymbol{\tau}_T^{i+1}}{\|\boldsymbol{\tau}_T^{i+1}\|} - \mu\mathbf{n}\right) && \text{contact with sliding.}
\end{aligned} \tag{26}$$

4.1. Non-smooth formulation of the contact law and shock law

At the local stage, contact reactions are computed from the values of the relative velocities, which have been calculated during the global stage. Newton's second law is used to determine for each particle the resulting acceleration and velocity, which are then integrated in time to find the new particle states. However, in the case of collisions between the bodies Ω_k, the relative velocity of an impacting particle is discontinuous and energy is dissipated. Furthermore, contact forces have to be replaced by impulsive forces to allow an instantaneously change of the velocity. Therefore, Eq. (5) which have been established in the case of a smooth evolution of the rigid bodies Ω_k constituting the system Σ, should be conveniently modified to take into account the dissipation occurring during collisions. This difficulty can be solved with the formalism of the NSCD method [4]. With this formalism, (5) becomes for two bodies subjected to contact:

$$\mathbf{M}(\dot{\mathbf{q}}^+ - \dot{q}^-) = \mathbf{F}dt + \sum_c \mathbf{P}\mathbf{s}. \tag{27}$$

where $\dot{\mathbf{q}}^+ = \mathbf{P}\dot{\mathbf{u}}^+$ and $\dot{\mathbf{q}}^- = \mathbf{P}\dot{\mathbf{u}}^-$ denote respectively the generalized coordinates after and before the shock, $\mathbf{s} = \mathbf{r}dt$ the contact impulsion measures, and dt the time interval considered. This frictional contact law is adapted to take into account of the collision by introducing the local average velocity $\tilde{\mathbf{u}}$ in Moreau's sense [4]:

$$\tilde{\dot{u}}_n = \frac{\dot{u}_n^+ + e_n\dot{u}_n^-}{1+e_n}, \qquad \tilde{\dot{\mathbf{u}}}_T = \frac{\dot{\mathbf{u}}_T^+ + e_T\dot{\mathbf{u}}_T^-}{1+e_T}, \tag{28}$$

This formal velocity, which corresponds to the real velocity if the evolution is smooth, enables one to take account of the friction during the shocks and of the propagation of these shocks in the granular medium. It depends on a normal and a tangential coefficient of restitution, e_n and e_T respectively.

5. Algorithm of resolution

For the solution of the problem, the time interval $[0, T]$ of the study is split into time interval h and the solution is obtained by solving successive finite-step problems on h. For each iteration, two stages are performed. The three key parts of the NSCD version of the DEM MULTICOR software developed are:

- A search algorithm used to construct a particle near-neighbor interaction list. In order to reduce the size of the non-smooth problem, only established or potential contacts are considered. For this aim, one considers a restricted list of candidates to the contact, called selected candidates. The method of selection uses a connection table [12].
- A local stage where collisional forces for each collision are estimated using the discrete contact law (22).
- A global stage where all collisional and other forces acting on the particles are summed and the resulting equation of motion (27) is integrated.

5.1. Global stage

Newton's second law is used to determine, for each particle, the resulting acceleration, which is then time-integrated to find the new positions of the particles. This process is repeated until the simulation is achieved. More precisely, it can be decomposed into the following steps:

- Prediction of the generalized coordinates $\mathbf{q}_m$ on the mean time step t_m. Starting with the values of $\mathbf{q}_n$ and $\dot{\mathbf{q}}_n$ given at the time step t_n:

$$t_m = t_n + \frac{1}{2}h \quad \text{and} \quad \mathbf{q}_m = \mathbf{q}_n + \frac{1}{2}h\dot{\mathbf{q}}_n. \tag{29}$$

- Computation of the generalized velocities $\dot{\mathbf{q}}_{n+1}$ at time step t_{n+1} by integration of Newton's second law:

$$\dot{\mathbf{q}}_{n+1}^{i+1} = \dot{\mathbf{q}}_n + \mathbf{M}^{-1}\left(h\mathbf{F} + \sum \mathbf{P}\mathbf{s}^{i+1}\right). \tag{30}$$

The exponent $^{i+1}$ means that the computation of $\dot{\mathbf{q}}_{n+1}^{i+1}$ is linked to those of $\mathbf{s}^{i+1}$ which is calculated in another iterative process (the local predictor-corrector scheme) until the convergence is achieved.

5.2. Local stage

After updating the relative velocities $\tilde{\mathbf{u}}$ at the contacts using relations defined in Section 2.1, a new estimation of the impulsion $\mathbf{s}^{i+1}$ is computed by using the finite-step frictional contact law. Thus, with the formalism of the NSCD method, the local scheme of predictor-corrector (22) becomes (31). For each particle, first the value of $\mathbf{s}^0$ is initialized to zero. Then starting from the value of $\mathbf{s}^i$ at step $i \geq 0$, the contact impulsions $\mathbf{s}^{i+1}$ at step $i+1$ are computed with the following local predictor-corrector scheme:

$$\begin{array}{ll} \text{predictor}: & \boldsymbol{\tau}^{i+1} = \mathbf{s}^i - \rho[\tilde{\tilde{\mathbf{u}}}_T^{\,i} + (\tilde{\tilde{\mathbf{u}}}_n^{\,i} + \mu\|\tilde{\tilde{\mathbf{u}}}_T^{\,i}\|).\mathbf{n}], \\ \text{corrector}: & \mathbf{s}^{i+1} = \text{proj}(\boldsymbol{\tau}^{i+1}, K_\mu), \end{array} \tag{31}$$

where the formal velocities $\tilde{\tilde{\mathbf{u}}}$ are defined in (28). Updating $\tilde{\tilde{\mathbf{u}}}$, let us note that only the value of $(\dot{\mathbf{u}}^+)^{i+1}$ after the shocks changes during the iterations, because linked to $\dot{\mathbf{q}}_{n+1}^{i+1}$ by (30). The relative velocity $\dot{\mathbf{u}}^-$ before the shocks remains constant, because linked to $\dot{\mathbf{q}}_n$. A crucial point is to decide when the local iterative procedure converges. So as to decrease the iteration number of the local scheme, we use as criterion of convergence the following error estimator in constitutive law, based on the "violation" of the contact bi-potential [13]:

$$\epsilon = \sum b_c(-\tilde{\tilde{\mathbf{u}}}^{i+1}, \mathbf{s}^{i+1}) + \tilde{\tilde{\mathbf{u}}}^{i+1}.\mathbf{s}^{i+1}, \tag{32}$$

where the sum carries on active contacts. This quantity is always positive and equal to zero when the couple of dual variables is extremal (when the contact law is exactly satisfied).

This kind of error estimator was proposed first by Ladevèze [14] in order to assess Finite Element computations. In order to obtain finite values of the bi-potential (15), which contains indicatory functions, the impenetrability and friction conditions have to be enforced prior to calculate the error [13]. The global stage and the local stage are successively applied until convergence is reached. Finally, the generalized velocities are obtained using relations defined in Section 2.1 and the generalized coordinates are updated according to:

$$\mathbf{q}_{n+1} = \mathbf{q}_m + \frac{1}{2}h\dot{\mathbf{q}}_{n+1}. \tag{33}$$

6. Numerical simulation with MULTICOR

In the following examples of dynamics simulations, the computations are made with the extension in 3D of the MULTICOR software [15]. This software is based on the Non-Smooth Contact Dynamics (NSCD) method and the contact bi-potential formalism presented above. We have focused our attention on examples representative of the capabilities of MULTICOR. The particles as well as the boundaries are assumed to be perfectly rigid. Each particle is subjected to the gravitation force and to the contact force resulting from neighborhood particles and boundaries.

6.1. Discharge of a silo with inclined bottom

This example presents the discharge of a silo constituted of 1000 spherical particles with a radius of 5 mm, subjected to gravity and contact forces (Fig. 4). The friction coefficient is equal to 0.2, $e_n = 0$ and $e_T = 1$. The time step is $h = 10^{-3}$ s. Granular flows, such as the movement during the discharge of material from a hopper are of special interest in materials handling. Firstly, we study the evolution of potential and effective contacts. An effective contact is a contact with impulse value higher than zero. In Fig. 5, we clearly observe different stages during the discharge of the silo. Firstly, at the beginning of the simulation when the discharge is quasi-static (Fig. 4(a)), we observe that the the number of potential and effective contacts is very close. After the beginning of the turbulent flow where we observe a short but important difference between potential and effective contacts, we can see a constant gap during the discharge. The number of contacts decreases during the

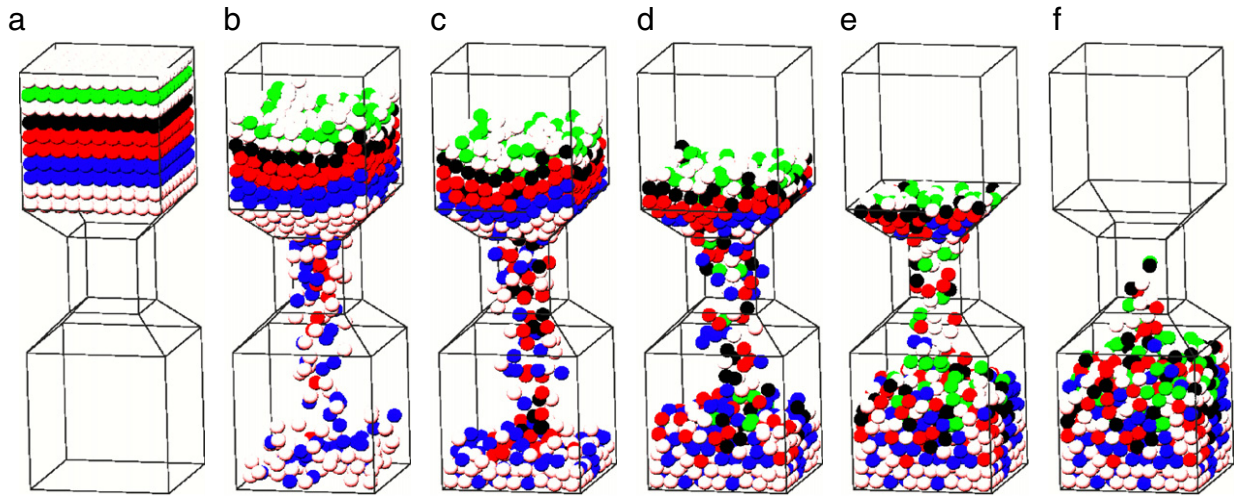

Fig. 4. Discharge of a silo with inclined bottom.

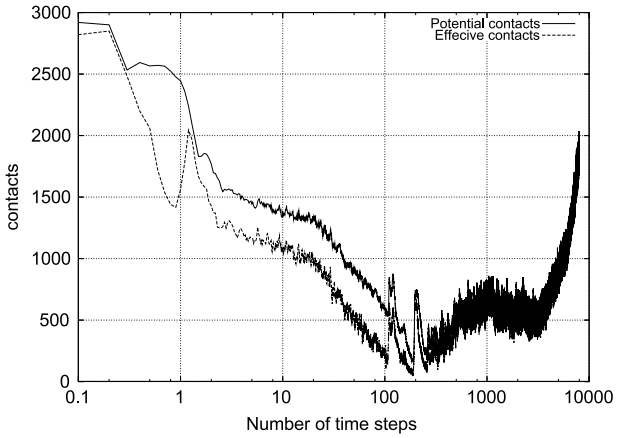

Fig. 5. Evolution of potential and effective contacts during the discharge of the silo.

particles falling until the formation of a particle pile at the bottom of the silo (Fig. 4(b)). During the formation of the pile the number of contacts swiftly increases and the difference between potential and effective contacts is very small because we find again a static stage. Fig. 6(a) and (b) show the evolution of the CPU time with the number of particles and the coefficient of friction respectively. We can observe a non-exponential evolution of the computation time. Therefore, we can use the proposed method for the simulation of large granular media. We can notice that the CPU time used for the detection phase of potential contacts is always less than 2% of the global CPU time. More than 96% of the global CPU time arises from the computation of impulses. This result prove the efficiency of the method used to select the restricted list of candidates to the contact [12]. In order to highlight the influence of the coefficient of friction μ, Fig. 7 shows the evolution of the number of effective contacts at the bottom of the silo with μ for the same time during the discharge flow of the silo. We can see that the flow of particles is less important when μ increases. From Fig. 4, we observe that during the discharge of the silo, the particles in the middle of the pile go down more quickly than the other particles. This phenomenon is in accordance with observations in a silo.

6.2. Formation of a pile of particles

This example allows to describe the formation of a pile of particles from the discharge of a silo constituted of 5600 spherical particles with different radii, only subjected to gravity and contact forces (Fig. 8). The friction coefficient is equal to 0.6, $e_n = 0$ and $e_T = 1$. The time step is $h = 5\,10^{-3}$ s. In order to avoid the dispersal of the first particles touching the floor, we block the velocity of the particles in contact with the floor. This simulation enables to highlight a well-known phenomenon during the formation of a sand pile. Indeed, experimental results show that the pressure under the sand pile is minimal in the middle of the contact surface [16]. This pressure hole phenomenon can be explained by the propagation of the chain forces during the formation of the pile. Fig. 9 shows that the simulation enables this important phenomenon

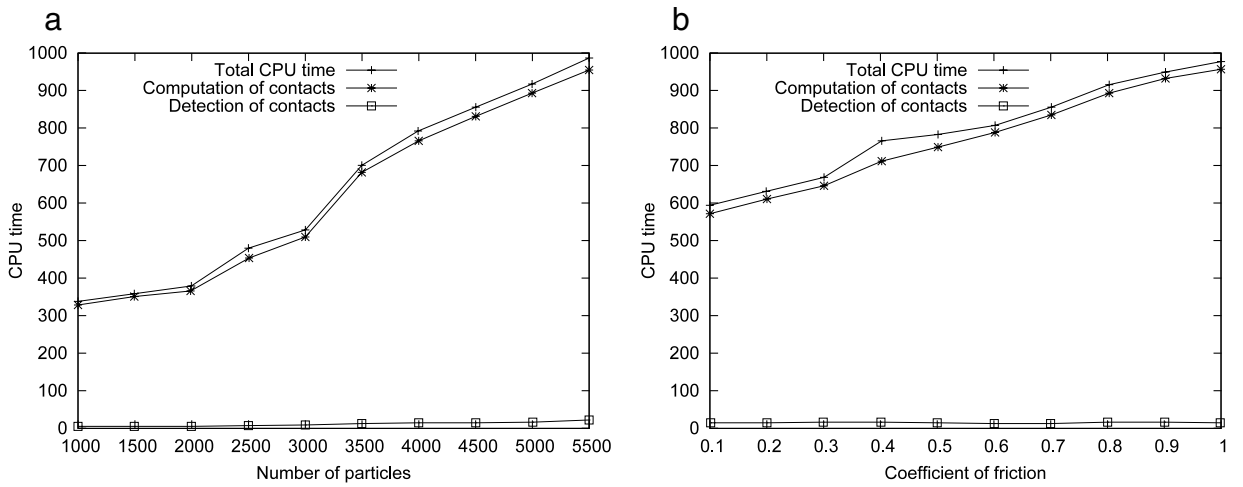

Fig. 6. (a): Evolution of the CPU time with the number of particles, (b) Evolution of the CPU time with the coefficient of friction.

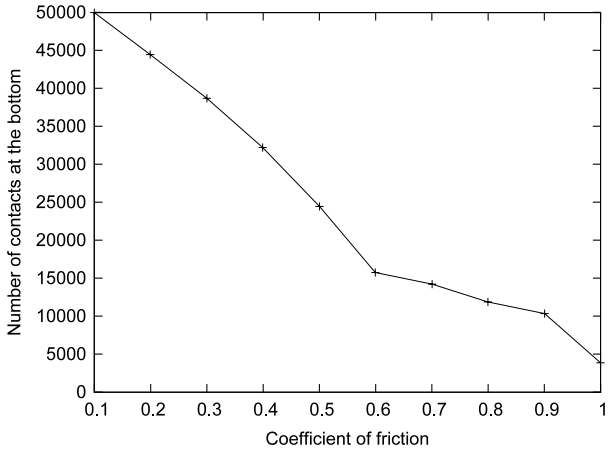

Fig. 7. Evolution of the number of effective contacts at the bottom of the silo at the same time during the discharge flow of the silo.

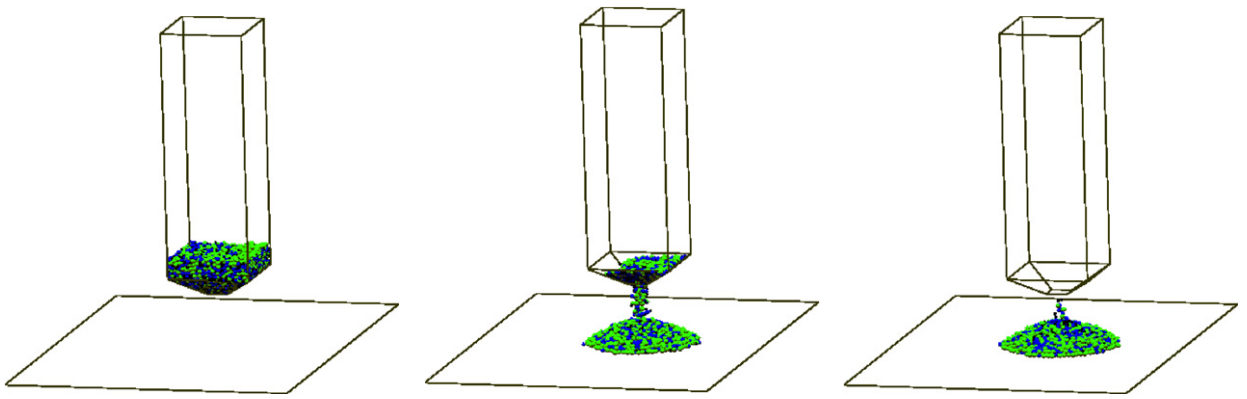

Fig. 8. Formation of a pile of particles.

to be described. We notice that this phenomenon disappears when considering the pressure under a regular canon-ball arrangement (Fig. 10(a)). Indeed for this regular arrangement, the chain of forces is homogeneous and the pressure under the pile displayed an expected form with a maximum of pressure in the middle of the contact surface (Fig. 9(b)).

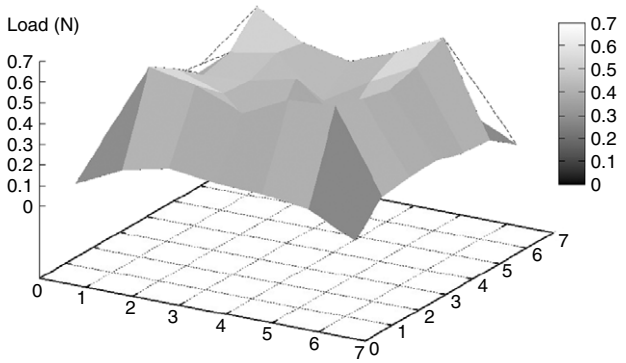

Fig. 9. Pressure under the sand pile.

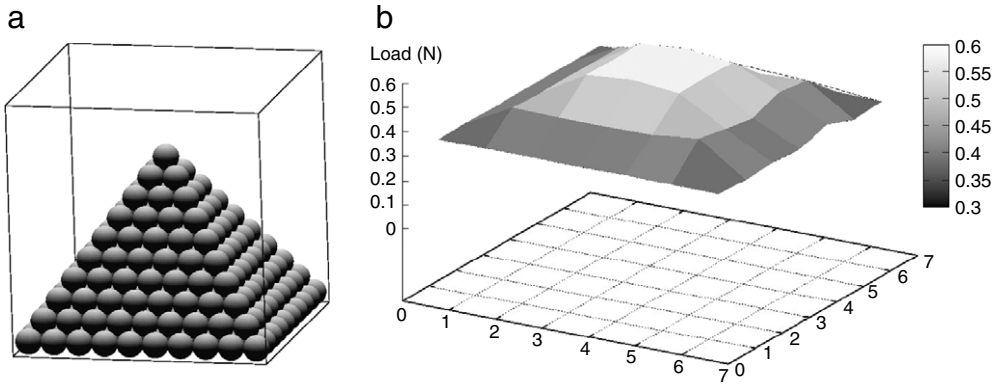

Fig. 10. (a): Regular canon-ball arrangement, (b): Pressure under the pile.

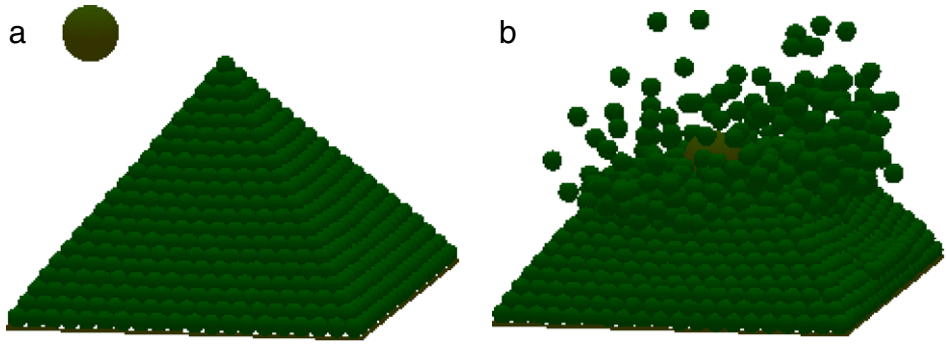

Fig. 11. (a): Regular canon-ball arrangement, (b): Impact on the pile.

6.3. Impact of a particle on a canon-ball arrangement

This example enables to observe the behavior of a canon-ball arrangement after the impact of a bigger particle (Fig. 11). The friction coefficient is equal to 0.2, $e_n = 0$ and $e_T = 0$. The time step is $h = 5\ 10^{-4}$ s. The velocity of the bigger particle is 5 m/s.

6.4. Granular segregation and Brazil nut effect

Segregation of particles in granular media is a common problem in the chemical and pharmaceutical industries and in materials processing. Vertical shaking of a mixture of small and large particles can lead to segregation and the so-called Brazil nut effect where the large particles accumulate at the top [17]. In this example, we report numerical results on the segregation of a vertically shaken mixture of 960 particles with different diameters (1.6 mm, 1.8 mm and 2 mm,). The particles are shaken sinusoidally in a rectangular box with an amplitude A and a fixed frequency $f = 28$ Hz. The friction

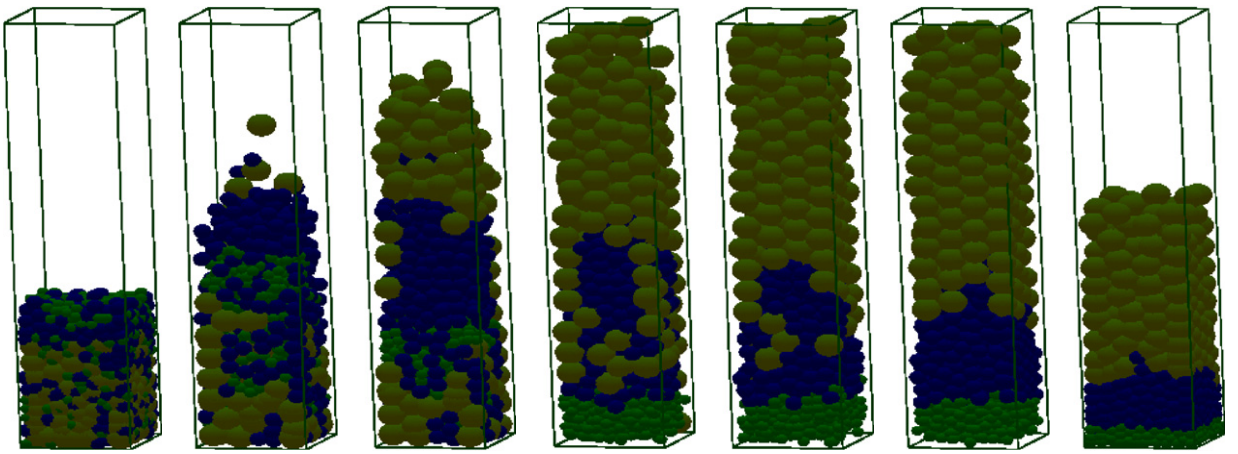

Fig. 12. Granular segregation.

coefficient is equal to 0.5, $e_n = 0$ and $e_T = 0$. The time step is $h = 5\ 10^{-4}$ s. The mixture is shaken during 20 s. Fig. 12 shows that the simulation exhibits a Brazil nut effect where all of the large particles accumulate at the top of the sample.

7. Conclusion

In this paper, we have presented an improved Discrete Element Method in 3D based on the Non Smooth Contact Dynamics and the bi-potential concept. The interaction law is described by Coulomb's unilateral contact law with dry friction in the framework of the bi-potential theory. This leads to an easy implementation of a predictor-corrector scheme involving just an orthogonal projection onto the friction cone. The numerical simulations presented have been made with the extension in 3D of the MULTICOR software developed by using this improved DEM. The numerical examples show the convergence and the robustness of our algorithm to model correctly the behavior of granular materials in complex three-dimensional problems, even in presence of numerous multiple contacts.

References

[1] P.A. Cundall, A computer model for simulating progressive large scale movements of blocky rock systems, in: Proceedings of the Symposium of the international Society of Rock Mechanics, vol. 1, pp. 132–150, Nancy, France, 1971.
[2] P.A. Cundall, O.D.L. Strack, A discrete numerical model for granular assemblies, Géotechnique 29 (1979) 47–65.
[3] M. Jean, Frictional contact in collections of rigid or deformable bodies: Numerical simulation of geomaterial motions, in: A.P.S. Selvadurai, M.J. Boulon (Eds.), Mechanics of Geomaterial Interfaces, Elsevier Sciences Publishers B.V., 1995, pp. 463–486.
[4] J.J. Moreau, Some numerical methods in multibody dynamics: Application to granular materials, Eur. J. Mech, A Solids 13 (1994) 93–114.
[5] C.H. Glocker, F. Pfeiffer, Multibody Dynamics with Unilateral Contacts, Wiley, New York, 1996.
[6] F. Pfeiffer, M. Foerg, H. Ulbrich, Numerical aspects of non-smooth multibody dynamics, Comput. Methods Appl. Mech. Engrg. 195 (2006) 6891–6908.
[7] G. de Saxcé, Une généralisation de l'inégalité de Fenchel et ses applications aux lois constitutives, C. R. Acad. Sc. Paris (1992) 125–129. t. 314, série II.
[8] P. Alart, A. Curnier, A mixed formulation for frictional contact problems prone to Newton like solution methods, Comput. Methods Appl. Mech. Engrg. 92 (1991) 353–375.
[9] J. Fortin, Simulation numérique de la dynamique des systèmes multi-corps appliquée aux milieux granulaires, thèse, Université de Lille I, 2000.
[10] G. de Saxcé, Z.-Q. Feng, The bipotentiel method: A constructive approach to design the complete contact law with friction and improved numerical algorithms, Math. Comput. Modelling 28 (1998) 225–245.
[11] A. Klarbring, Mathematical programmming and augmented lagrangien methods for frictional contact problems, in: A. Curnier (Ed.), Proc. Contact Mechanics Int. Symp., PPUR, 1992, pp. 409–422.
[12] J. Fortin, P. Coorevits, Selecting contact particles in dynamics granular mechanics systems, J. Comput. Appl. Math. 168 (2004) 207–213.
[13] J. Fortin, O. Millet, G. de Saxcé, Numerical simulation of granular materials by an improved discrete element methodn, Int. J. Numer. Methods Engrg. 62 (2005) 639–663.
[14] P. Ladevèze, Mécanique non linéaire des structures: Nouvelle approche et méthodes de calcul non incrémentales, Hermés, Paris, 1996.
[15] I. Sanni, Modélisation et simulation bi et tri-dimensionnelles de la dynamique unilatérale des systèmes multicorps de grandes tailles: Application aux milieux granulaires, thèse, Université de Picardie, 2006.
[16] G. Ovarlez, Statique et rhéologie d'un milieu granulaire confiné, Thèse de Doctorat de l'Université de Paris XI Orsay, 2002.
[17] A. Rosato, K.J. Standburg, F. Prinz, R.H. Swendsen, Why the Brazil nuts are on top: Size segregation of particulate matter by shaking, Phys. Rev. Lett. 58 (1987) 1038–1040.